7 Extrusion Equipment for Reactive Blending

Tadamoto Sakai

The use of polymer processing equipment to conduct reactive processes, particularly reactive blending, creates new and complex demands. Screw type extruders, in particular twin screw extruders, are the preferred devices for reactive blending but must be configured to address the major issues of required residence time, temperature and morphology development. This chapter deals with extruder design to provide the necessary reaction temperature and residence time, intensity of mixing, and devolatilization to remove by-products and residual reactants. Furthermore, the visualization techniques to observe morphology development during reactive blending in a twin screw extruder and on-line monitoring methods are described.

7.1 Extruders Used for Reactive Blending

The major equipment for manufacturing various kinds of polymer alloys is a screw extruder. Screw extruders are practically classified into single and twin screw types. A single screw extruder is used mainly for diversified thermoplastics processing, for example in blow molding, film and pipe extrusion, and injection molding. On the other hand, a twin screw extruder is generally used for blending and controlling the microstructure of a polymer alloy, and polymerization such as grafting [1–4]. Further, a reciprocating single screw extruder can be classified into the same categories as a twin screw extruder from the point of the mutual interaction between screw flight and barrel.

Twin screw extruders are usually defined by intermeshing type and rotational direction as shown in Fig. 7.1 [3]. Figures 7.2 to 7.5 show a non-intermeshing counter-

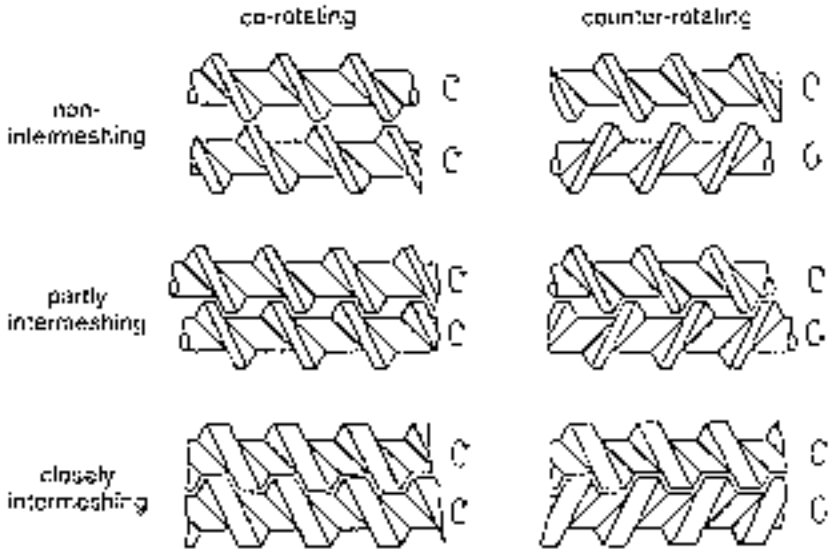

Figure 7.1 Twin screw extruders of various kinds

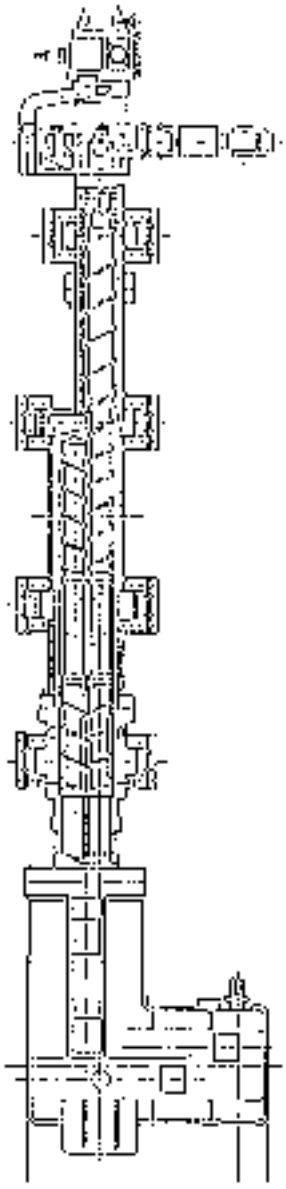

Figure 7.2 Typical non-intermeshed twin screw extruder with long L/D (tangential type)

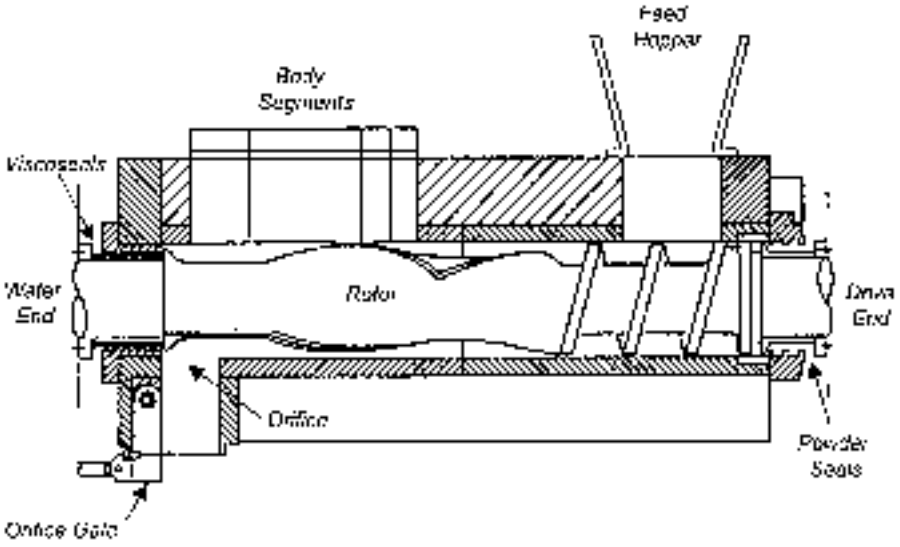

Figure 7.3 Non-intermeshed counter-rotation twin screw extruder with short L/D (Farrel Continuous Mixer)

rotational twin screw extruder with long L/D (manufacturer: Welding, JSW), a non-intermeshed one with short L/D (manufacturer: Farrel, JSW, Kobe Steel), an intermeshed co-rotational one with segmented barrels and screws (manufacturer: Werner & Pfleiderer, Berstorff, JSW, Toshiba Machinery, Davis-Standard and many other manufactures in the world), and a reciprocating type single screw extruder (manufacturer: Buss), respectively. An intermeshed counter-rotation twin screw extruder with segmented screw and barrels (manufacturer: JSW, Leistritz) is also used for reactive blending as well as an intermeshed co-rotating design.

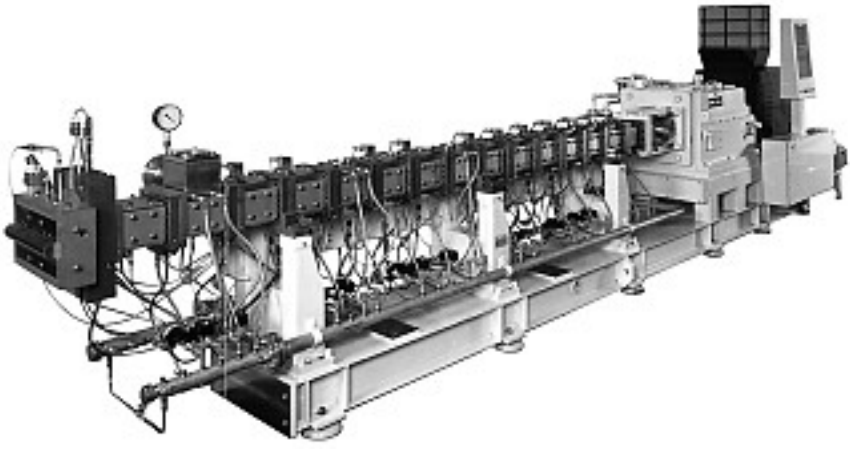

Figure 7.4 Intermeshed co-rotational twin screw extruder with segmented barrel and screw (JSW TEX)

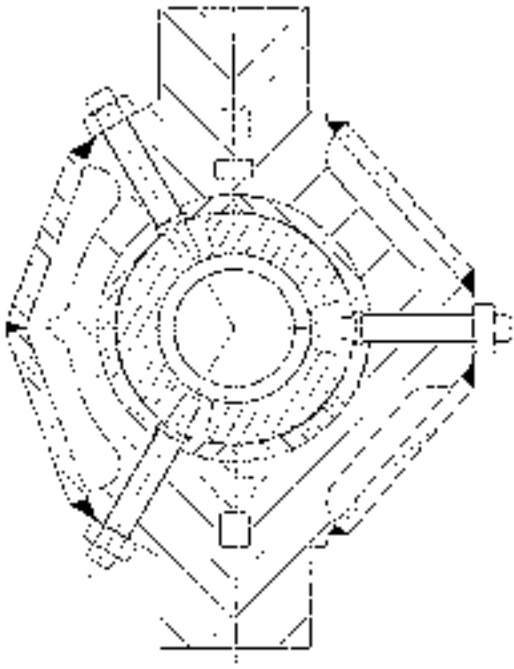

Figure 7.5 Reciprocating single screw extruder (Buss, Ko-kneader)

Recently, comparisons among these various kinds of twin screw extruders have been made [4–7]. Table 7.1 illustrates the results of the comparisons among twin screw extruders. Depending on operational purposes, the most appropriate extruder should be selected. In general, however, intermeshed co-rotational twin screw extruders are widely

Table 7.1 Comparisons of Functional Characteristics of Different Twin Screw Extruders

	Low speed corotating	High speed corotating	Low speed ctr-rotating	High speed ctr-rotating	Tangential ctr-rotating
Throughput	+	++	+	+	++
Distributive mixing	+	++	+	+	++
Dispersive mixing	*	+	*	++	−
Degassing	*	+	+	++	+
Melting	+	+	+	++	+
Conveying	+	*	++	+	−
Self-wiping	+	++	+	*	−
Screw speed	−	++	*	+	++
RTD width	+	*	++	+	*
Pressure development	+	*	++	+	−
Screw separation	−	+	*	*	+
Feed capability	+	*	++	++	+

RTD: Residence time distribution; ctr: counter; ++ = very good; + = good; * = fair; − = poor.

used for diversified purposes, mainly because of their flexible mixing capability over wide ranges, the self-wiping effect and a great deal of accumulated operational experiences in the plastic industry. On a laboratory-scale, small screw diameter twin screw extruders such as 25–30 mm are commonly utilized. The 45–65 mm twin screw extruders are used for bench-scale production while 65–150 mm for industrial scale units are widely used in reactive blending applications. For even larger scales, more than 150 mm twin screw extruder are applied (max. 400 mm).

7.2 Mixing Mechanism

Mixing effects play the most important roles in reactive blending using various screw type extruders. Almost all polyblends are prepared under very high melt-viscosity conditions, and therefore reactive blends are strongly dominated by diffusion-base reactions among reactants, compatibilizers and polymeric components.

The effect of the mixing action in a screw channel is usually analyzed in the two different categories of ''distributive mixing'' and ''dispersive mixing''. The former is mainly governed by shear rate γ' and shear strain γ. On the other hand, the latter is determined by the degree of shear stress σ, specific energy $E_{sp.}$ and extensional flow component. To control these mixing effects, many kinds of mixing elements are used in each twin screw extruder. For example, in the case of an intermeshed co-rotational twin screw extruder, segmented kneading disks (Fig. 7.6) are commonly utilized. These kneading devices are defined by the number of lobes (usually two or three), disk width and length, tip clearance and stagger angle (right or left handed, neutral). Using these design parameters one can control the effects on mixing, polymer temperature and filling pressure in a twin screw extruder.

Figure 7.7 shows the qualitative effects on dispersive and distributive mixing when different kneading disks design features are utilized [8]. To increase distributive mixing,

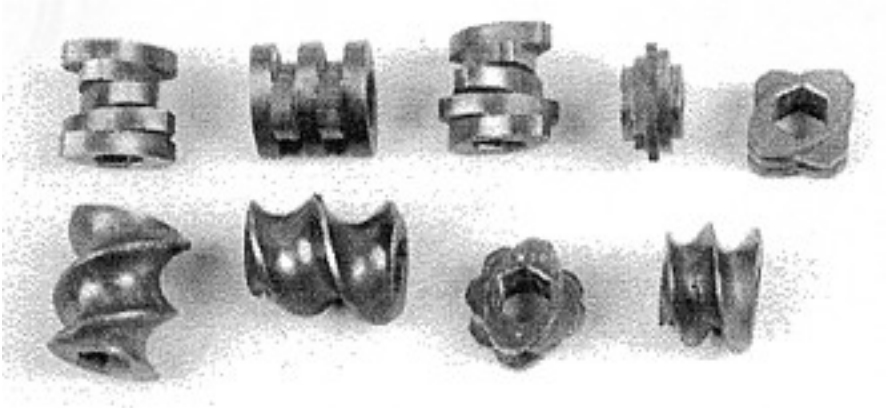

Figure 7.6 Examples of conveying and kneading disk elements

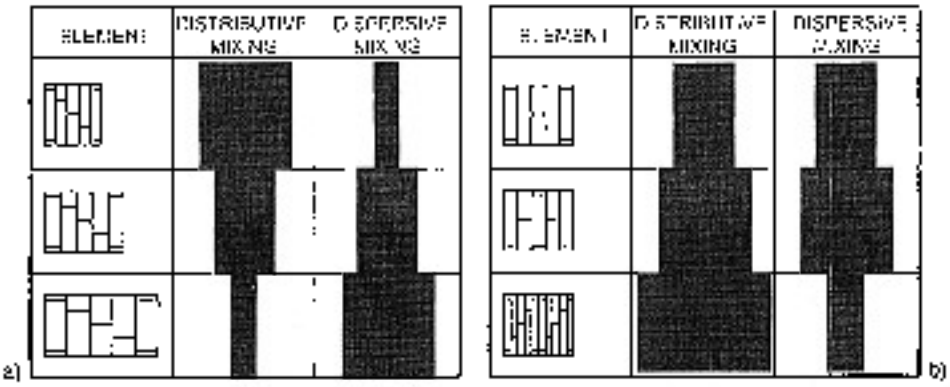

Figure 7.7 Kneading elements: (a) Effect of disk width on distributive and dispersive mixing; (b) effect of disk stagger on distributive and dispersive mixing

furthermore, specially designed mixing elements such as turbine type and throttle valves attached on the barrel for pressure regulation are preferably used. In many cases, it is very important how the screw geometries are designed so as to achieve greater mixing effects without excessive polymer temperature rise.

7.2.1 Distributive and Dispersive Mixing

7.2.1.1 Distributive Mixing

The distributive mixing between two components with high viscosity is determined by a laminar mixing flow. In this laminar mixing, molten polymer components in the flow field are deformed due to the shearing force. As a result of the deformation, the striation thickness M between two molten polymer components can be reduced. A smaller striation thickness M results in better distributive mixing in the laminar flow field [9]. The striation thickness M is calculated by using the following equation when the melt viscosity difference between two components exists in the shear flow field.

$$M = (l_d/\gamma\phi_d)(\eta_d/\eta_m) \tag{7.1}$$

where

l_d = length of a cube as a smaller component
ϕ_d = volume fraction of a smaller component
η_m = melt-viscosity of a matrix component
η_d = melt-viscosity of a domain component
γ = shear strain (product of shear rate and average residence time)

From Eq. (7.1) we can easily recognize that larger shear strain γ contributes to better mixing. For improving distributive mixing, we generally design for higher shear rate, which means higher screw speed and/or shallower channel depth, instead of longer

residence time (if reaction time is sufficient to complete). The distributive mixing is further enhanced by forcing the laminar flow field through reorientations.

7.2.1.2 Dispersive Mixing

In the case of dispersive mixing, larger shear stresses and extensional forces in a flow field should be imposed if the break-up of agglomerates and droplets of each polymeric component are required [10, 11]. Recent theoretical analyses concerning shear stress and extensional flow distribution in a twin screw extruder have made great progress [4, 10–14]. The simulation results suggest that the flow profiles in both the screw flight clearance and apex region in a twin screw extruder have great influence on dispersive mixing which, in turn, has a close relationship with the morphological development of a polymer alloy.

7.2.1.3 Viscosity Ratio and Surface Tension

The viscosity ratio (η_d/η_m) between the matrix (subscript m) and the domain (subscript d), and surface tension π play very important roles in the determination of droplet size. The minimum domain size d obtained by mixing is expressed by the following equation [15]:

$$d = (A\pi/\eta_m\gamma')\mathrm{f}(\eta_d/\eta_m) \qquad A = \text{constant} \tag{7.2}$$

Figure 7.8 [17] shows the relationship between the viscosity ratio of a polyamide-rubber binary blending system and the size of domain particles obtained by mixing and kneading with a twin screw extruder [16–18]. Generally, it is easier to obtain the fine domain size under conditions where the two melt viscosities are close. Furthermore, the domain size reduction easily occurs when the surface tension π between each polymer particle is low, even if there exists a considerable melt-viscosity difference. This means that both the addition of a compatibilizer or interfacial copolymerization reactions result in lower surface tension and, consequently, the domain size reduction is effectively accelerated. To analyze the domain size in polyblending, the Weber Number W_e or the following modified

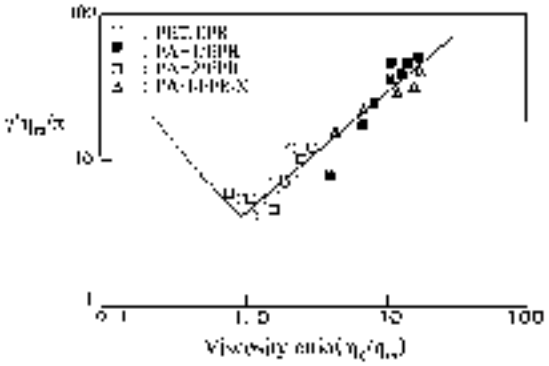

Figure 7.8 Dimensionless domain size as a function of melt viscosity ratio

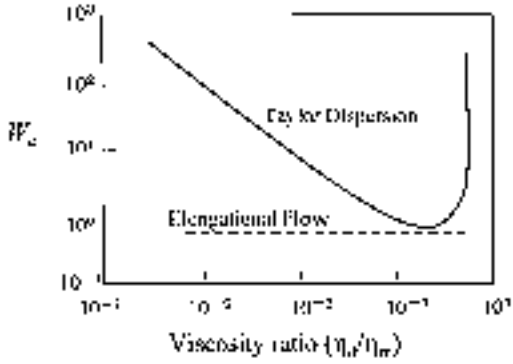

Figure 7.9 Dispersive process as a function of viscosity ratio

Weber Number W_e^* is often used [19].

$$W_e^* = \gamma' \eta_d \{1 - 4(\phi_d \phi_m)^{0.8}\}/\pi \tag{7.3}$$

where ϕ is a volume fraction of each component.

To develop and stabilize the optimum morphology of a polymer alloy, it is very important to utilize a particular interfacial chemical reaction or a pre-designed compatibilizer to improve the surface tension or interaction between the domain and matrix polymeric components, as well as to select of the optimum operational conditions for mixing [17, 20, 21]. For operating conditions, the larger the W_e or W_e^*-value (that is, higher shear rate) becomes, the smaller the domain size which can be obtained.

7.2.1.4 Extensional Flow

It is well recognized that extensional flow is advantageous to deform and break up droplets with large viscosity difference. As shown in Fig. 7.9 [22], shear flow can lead to the droplet break-up only under the condition of a viscosity ratio of up to 3.8. This suggests that one should utilize sufficient extensional flow as well as high shear flow [22]. For this reason, the simulation of extensional flow to obtain the optimum screw design and the use of an additional, extensional mixer are considered as significant tools [23].

7.2.2 Dissipative Melting

The maximum shear stress, accompanied with frictional and extensional forces, in a reactive blending process is usually generated at the melting zone of a screw extruder. In this melting region, each component is ground and dispersed as a result of undergoing strong dispersive mixing effects. Under dissipative melting each polymeric component changes into very small particles as droplets within a very short time, i.e., 0.1–10 s. Figure 7.10 is a photo showing the deformation of semi-solid phase of polypropylene (PP) by receiving extremely large forces at the melting region of a screw channel [24]. The same experimental result for the great deformation in unmolten or incomplete molten phase before the completion of melting, can be obtained, especially in a twin screw extruder.

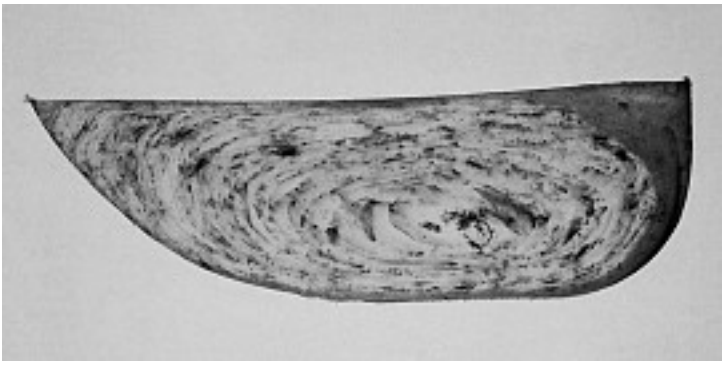

Figure 7.10 Solid phase deformation by strong shearing stresses in the melting region

This deformation at the melting zone plays a very important role, particularly in dispersive mixing. And dispersive mixing is closely related with the morphological development [5, 24, 25].

Some experimental results on the observation of the melting behavior of high density polyethylene (HDPE) in an intermeshed counter-rotational twin screw extruder using so-called ''cooling experiments'' are shown in Figs. 7.11 and 7.12 [11, 25–27]. Figure 17.13 shows the typical melting process in a single screw extruder for reference. When comparing the melting process of a single screw and that of a twin screw extruder, the latter shows much more rapid melting and a more complex co-mingling of the solid and molten phases. Furthermore, the change of average domain size along each position of a twin screw extruder observed by a screw cooling technique is closely linked to the melting process [28, 29].

A generalized structure development model for an immiscible polymer alloy is shown in Fig. 7.14 [30–32]. The domain size of about 10 micron level is quickly attained from polymer pellets of 2–5 mm only at the final stage of melting. After the completion of

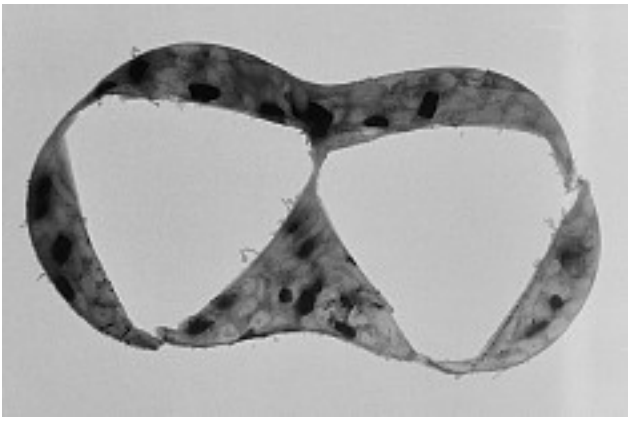

Figure 7.11 The start of melting behavior in an intermeshed co-rotational twin screw extruder (HDPE)

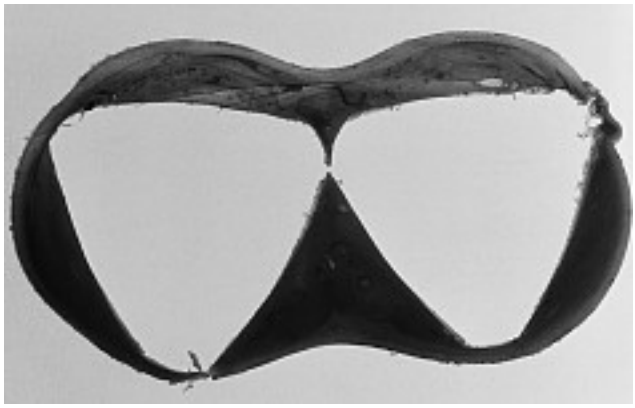

Figure 7.12 The end of melting behavior in an intermeshed co-rotational twin screw extruder (HDPE)

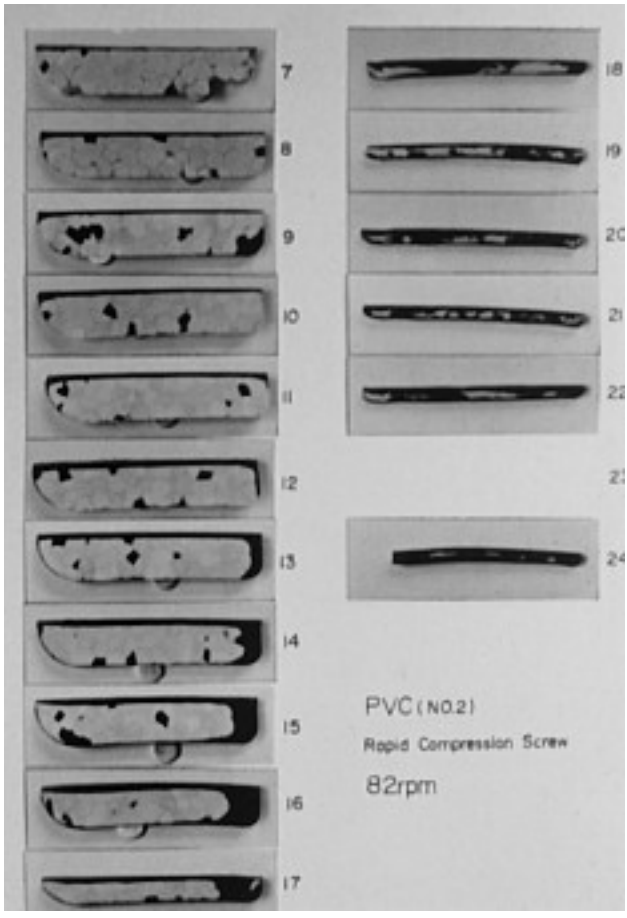

Figure 7.13 Melting process in a single screw extruder (soft PVC)

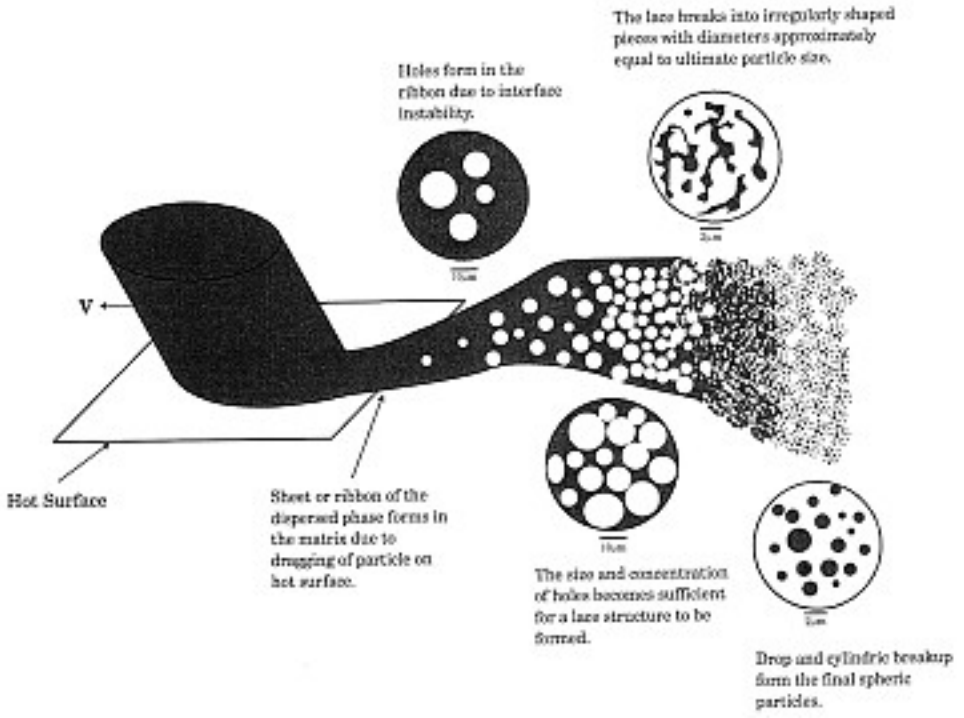

Figure 7.14 Morphology development model proposed by Macosko et al.

melting, the reduction of the domain size gradually progresses toward the exit by undergoing progressive distributive, dispersive and extensional mixing, and consequently the domain size at 1.0 micron level can be finally obtained.

Generally, the melting behavior in a twin screw extruder is very complicated as compared in a single screw extruder. If a simplified melting model is applied from the practical point of views the melting progress can be calculated, for example, by the following equations [33].

A mass balance is shown as follows from a mass of solid bed moving in the x_1 direction, having a screw channel height $H_s(x_1, x_3)$ and width $X(x_1)$,

$$dQ_s/dx_1 = -\rho_s \int_0 X(xi) v_{s2}(x_1, x_3)\, dx_3 \tag{7.4}$$

where v_{s2} is the velocity of the solid bed melt interface in ''2'' direction (depth), ρ_s is the density of the solid bed and Q_s is the mass flow rate. x_1 and x_3 are the helical and cross-sectional directions, respectively.

Considering the equations of continuity and motion using the hydrodynamic lubrication theory in the melt layer and, in addition, the heat flux from the melts into the solid melt interface, Eq. (7.5) is obtained:

$$v_{s2}(x_1, x_3) = [-\kappa_m(\partial T/\partial x_2)|_{x_2}^{melt} = H_m]/\rho_s\{C_s(T_m - T_0) + \lambda\} \tag{7.5}$$

where C, T and κ are the specific heat, temperature and thermal conductivity, and λ is the heat of fusion. The subscripts b, o, m and s refer to barrel, initial condition, melt layer, and solid bed, respectively.

Finally, the melting equation is shown as follows:

$$\mathrm{d}H_\mathrm{m}/\mathrm{d}x_1 = [h_\mathrm{b}(T_\mathrm{b} - T_\mathrm{m}) + 1/f_0\{U_1^2 + (f_2 f_0)/(f_2 f_0 - f_1^2)U_3^2\} + (\partial \mathrm{p}/\partial_\mathrm{x}1)^2\{(f_2 f_0 - f_1^2)/f_0\}]/\rho_\mathrm{s}\{C_\mathrm{s}(T_\mathrm{m} - T_0) + \lambda\}v_{\mathrm{s}0} \quad (7.6)$$

In Eq. (7.6) f and $v_{\mathrm{s}0}$ are given by the next expressions:

$$f = \int_0^{H_\mathrm{m}} (\mathrm{x_i}/\eta)\,\mathrm{d}x_2 \quad (7.7)$$

$$v_{\mathrm{s}0} = Q_\mathrm{s}/\rho_\mathrm{s}A_\mathrm{c}(2m - 1) \quad (7.8)$$

where A_c, h_b, m, and η are the cross-sectional area of the screw channel, heat transfer coefficient at the surface of inner barrel, number of the screw element, and melt viscosity of a polymer, respectively.

Figure 7.15 shows an example of calculated results on the melting and pressure generation in an intermeshing co-rotation twin screw extruder (screw diameter 30 mm), when low density polyethylene (LDPE) is used at a screw speed 200 rpm and feed rate 13.5 kg/h [33].

Recently the analyses on melting and flow are becoming common in screw extrusion. From these analyses on melting behavior, dispersive mixing effects in a twin screw extruder can be theoretically estimated to a certain extent [11]. Furthermore, the morphology development at the melting region of a single screw extruder has been calculated using a striation thickness theory [34], and a computational model incorporating

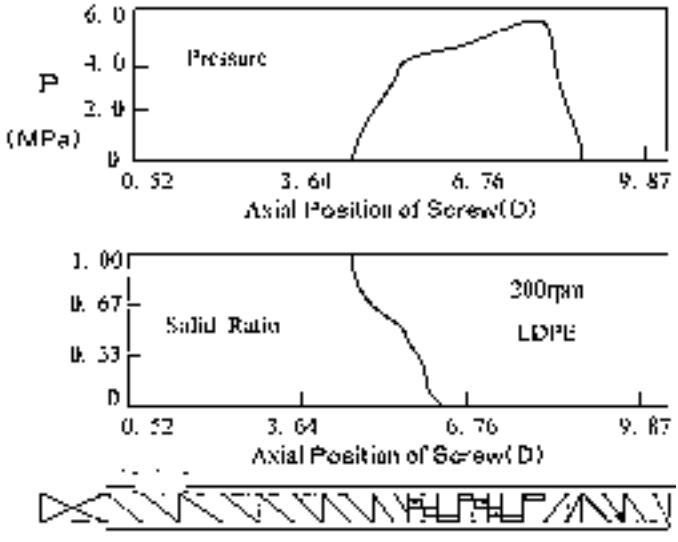

Figure 7.15 Simulation results on melting in co-rotation screws (LDPE)

the coalescence behavior has been developed for an intermeshed co-rotational twin screw extruder [35].

7.3 Residence Time and Residence Time Distribution

The residence time distribution of a screw extruder is basically sharp as shown in the comparisons between other reactors in Fig. 7.16 [36]. Depending on extruder type and screw design, the distributions can be controlled depending on the longitudinal mixing.

The average residence time is directly calculated from the available holdup volume divided by the volumetric flow rate. Owing to the improvement of mechanical design, machining, and metallurgical technology, twin screw extruders have moved in the

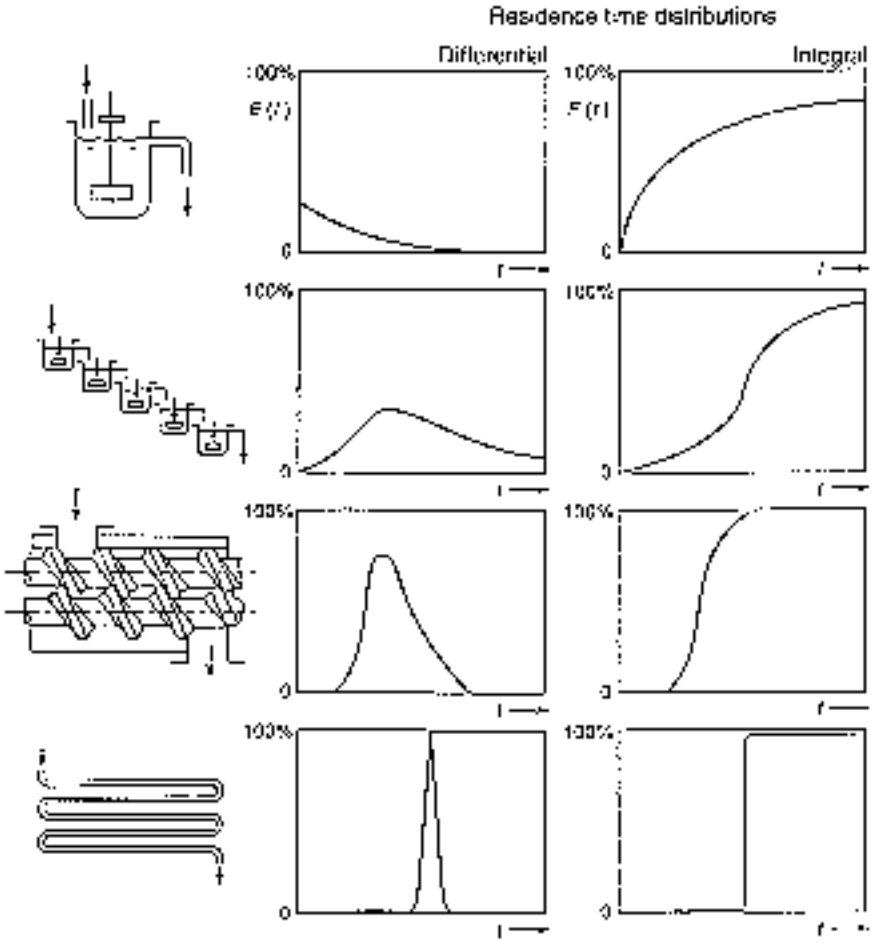

Figure 7.16 Comparison of various reactors' residence time distribution curves

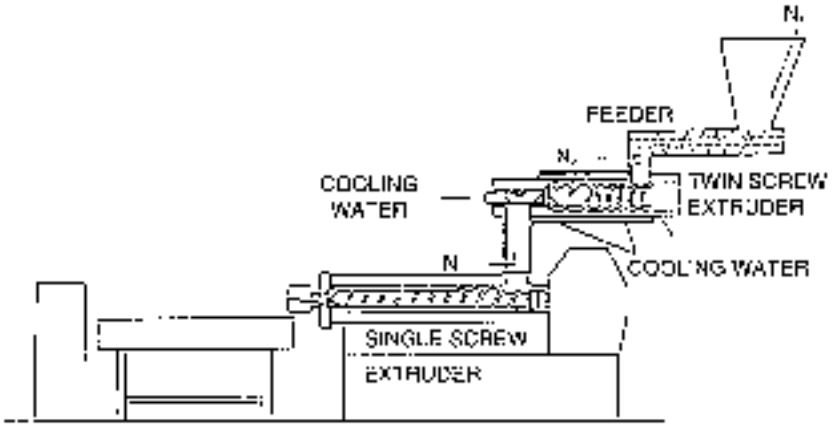

Figure 7.17 Two-step reactive extrusion system combined with twin screw extruder and single screw extruders

direction of deeper screw channels and lengths up to 65 L/D, particularly in the case of an intermeshed co-rotational twin screw extruder. On the other hand, single screw and non-intermeshed twin screw extruders are easily available at deeper screw channel depths and longer screw lengths (up to 100 L/D) than those of intermeshed types. As twin screw extrusion is usually carried out under starve feed conditions, one has to estimate the real holdup volume with calculation of the molten polymer fill length in the twin screw channels.

In general, residence time for chemical reactions can be controlled up to 10–30 minutes. From a practical point of view, however, one has to conduct these chemical reactions in less than a few minutes in the case of twin screw reactive blending extrusion. One of the solutions to increase residence time for chemical reactions is, for example, to combine a twin screw extruder having good distributive and dispersive mixing with a single screw extruder with longer residence time as shown in Fig. 7.17 [37].

7.4 Devolatilization

Devolatilization is one of the important functions in reactive blending. In order to improve the devolatilization of a residual monomer and/or by-products in chemical reactions, parameters such as screw speed, surface renewal (screw geometry, the addition of an accelerator; i.e., water), venting area, and output rate should be optimized. Generally, a counter-rotational twin screw extruder exhibits higher devolatilization efficiency, when compared with a co-rotational extruder with the same screw configurations as shown in Fig. 7.18 [38]. However, the advantage of a co-rotation type twin screw extruder widely used in the plastic industry is its self-wiping effects on preventing stagnant layers from thermal degradation at a venting zone.

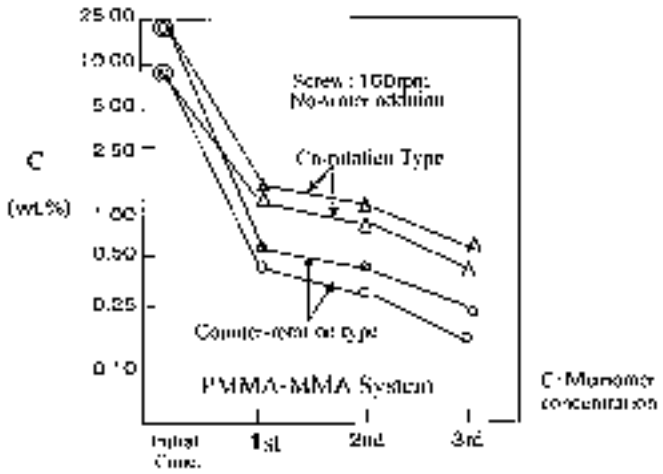

Figure 7.18 Effects of rotation direction on devolatilization

For easy understanding, Latinen's theory describing devolatilization in an extruder is shown as follows [39]:

$$\log(C_0 - C_E)/(C_L - C_E) = ASLN^{1/2}/Q \tag{7.9}$$

where C_0, C_E, and C_L are initial, equilibrium, and final concentrations of a degassing component in a polymer, respectively. Therefore, $(C_0 - C_E)/(C_L - C_E)$ shows the devolatilization efficiency. The terms A, L, N, Q and S are a constant, screw length, screw speed, output rate, and surface area of venting zones, respectively. However, Latinen's theory dealt with no transport effects, such as stripping and mixing. More precise and practical theories should be established. For example, the operational and/or design parameters are affected by the number of screw flights, screw pitch and the degree of fill at the venting zones [40].

The design of a venting hole is important in preventing the stagnation and back-flow of condensed volatile. Figure 7.19 shows the typical venting structure for an intermeshing co-rotational twin screw extruder. A special intermeshing co-rotation twin screw extruder (screw diameter: 256 mm) with 6 vent holes is shown in Fig. 7.20.

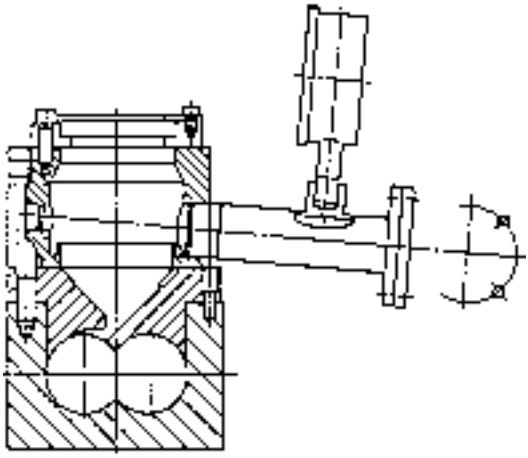

Figure 7.19 Typical vent hole structure for devolatilization operations

Figure 7.20 Intermeshing co-rotational twin screw extruder with 6 venting holes (JSW, TEX 250)

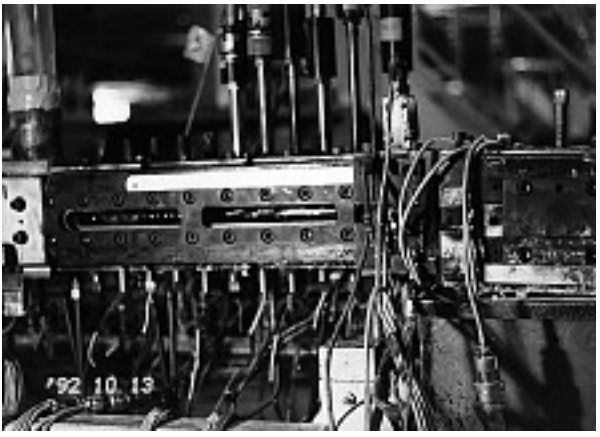

Figure 7.21 Visualization for melting and mixing through glass windows

7.5 Microstructure Development and Monitoring in Reactive Blending

Some visualization techniques used to observe dynamic melting and mixing behaviors directly are important in a practical sense. Figures 7.21 and 7.22 show some experimental results on the direct observation through a barrel with transparent glass windows [5, 41]. Hatch type and clamshell type barrels are also commercially available in order to facilitate easy removal of samples from a certain region of a twin screw extruder.

A more complicated mechanism of morphological development in a twin screw extruder has been considered in a reactive process in which chemical reactions play an important role. For the purpose of analyzing the morphological development in a single and/or twin screw extruder, some techniques such as sampling nozzle attachment are used.

Figure 7.22 Experimental results on visualization through a glass window

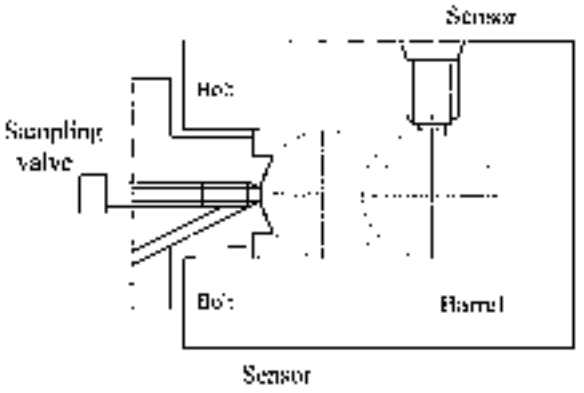

Figure 7.23 Structure of sampling nozzle/valve for analyzing morphology development

Figure 7. 23 shows the structure of a sampling nozzle. It enables the extraction of a small portion of the molten materials in real time, and the analysis of the progress of chemical reactions and morphology changes of each component [42]. Using this technique for analyzing the morphology development, two experimental studies are introduced.

First, Figs. 7.24 and 7.25 illustrate the experimental results when monitoring the morphology development in the case of a maleated polypropylene (mPP)-polyamide (PA) binary reactive blending system (where A-1: 1st kneading zone, A-2: intermediate, A-3: 2nd kneading zone, A-4: die exit).

In this study, a special technique was used to take molten samples directly from the desired position of a twin screw extruder (screw diameter: 30 mm) during the extrusion operation [41]. This experimental device, which was developed at JSW, is shown in Fig. 7.23. These results indicate that the PP particle size rapidly decreases at the melting zone

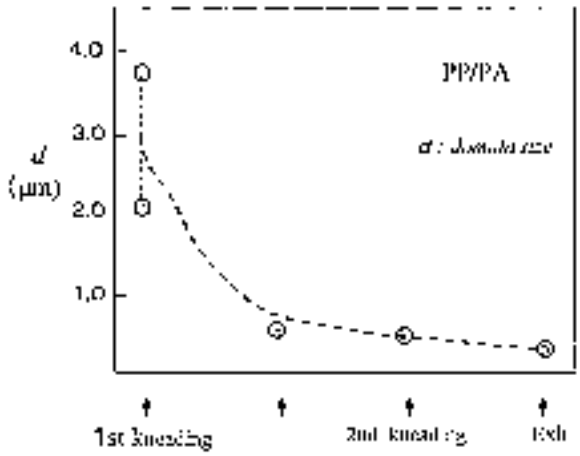

Figure 7.24 Morphological changes in twin screw reactive processing

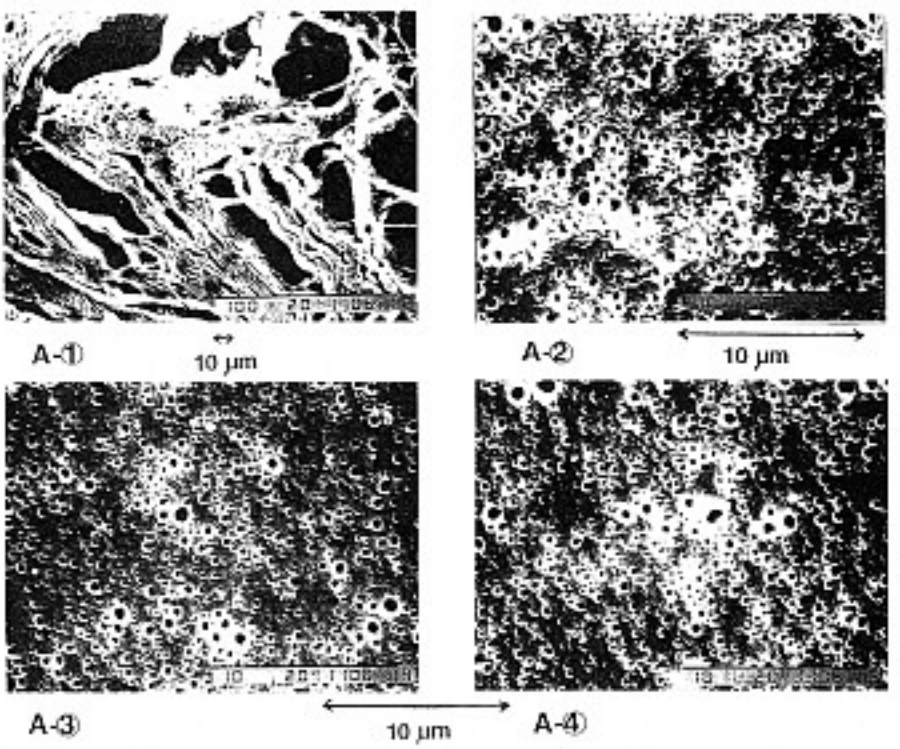

Figure 7.25 Morphology change in a twin screw extruder (mPP-PA binary blend system)

and then reduces relatively slowly through the melt-mixing zone. The rapid size reduction in the melting region was induced by large shear stresses and extensional forces, etc. generated in the twin screw extruder during dissipative melting. Furthermore, the stabilization of fine droplets is brought about by chemical reaction, which enables not only a decrease in surface tension π, but also the prevention of the coalescence among PP droplets. The domain size is strongly dependent on the concentration of the reactively formed, graft copolymer produced in blending [43]. The results are shown in Fig. 7.26.

Second, some interesting experimental results were reported on the micro-structure development of polyphenylene oxide (PPE)-PA-PP ternary blending system in an intermeshed counter-rotation twin screw extruder (screw diameter: 30 mm) using the same sampling technique. The results are shown in Fig. 7.27 [44] (where 1–6: from the start of melting in 1st kneading zone to 2nd kneading zone, 7: die exit). The multi-layered structure development, involving the so-called ''salami'' structure, can be clearly observed as a result of the phase inversion in a twin screw extruder.

New technology to evaluate the structure development in a twin screw extruder has been proposed, for example, an on-line monitoring apparatus on the microstructure change in real time during operation as shown in Fig. 7.28. In this system, the microstructure can

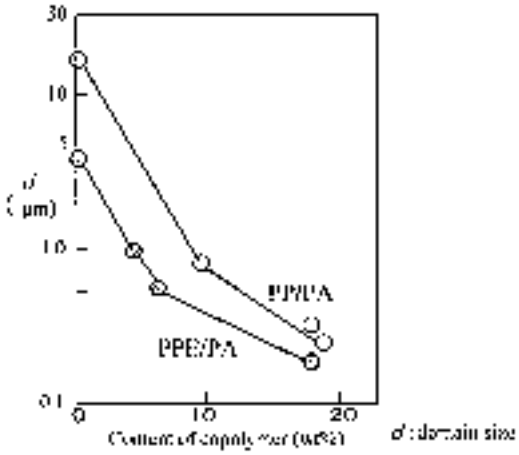

Figure 7.26 Relationship between copolymer content and domain size

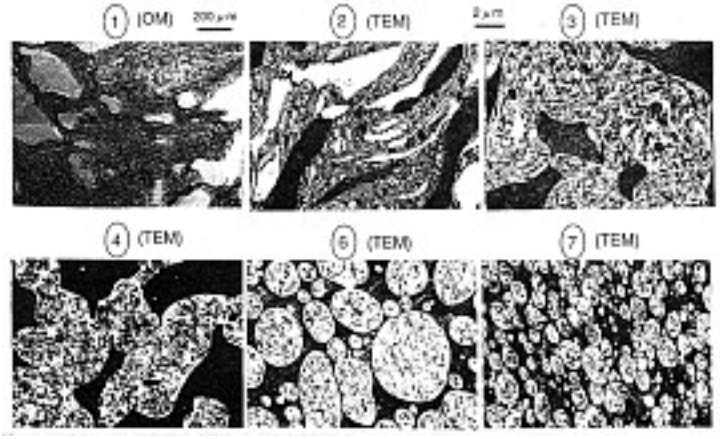

Figure 7.27 Morphological change of PPE/PA/PP ternary blends in the mixing process

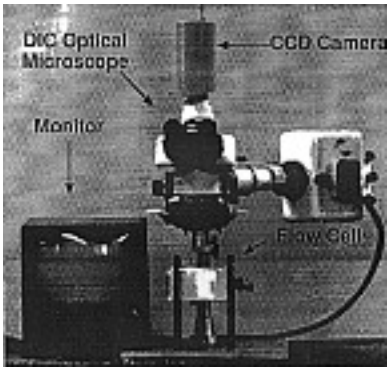

Figure 7.28 On-line optical bench for morphology analysis

be simultaneously analyzed using an image analysis technique [45]. In the near future these kinds of studies are expected to become more common and applied in industry.

7.6 Hybridized Polymer Processing Systems

A hybridized processing system to directly obtain a finished product can be an ideal process that can prevent undesirable phenomena like thermal degradation. The hybridized system, for example, which combines twin screw extrusion and injection molding, has the following advantages that are expected to be in practice in the near future:

1. Minimization of thermal degradation by direct molding/shaping.
2. Easy fixation and control of the morphology obtained from twin screw reactive blending.
3. Linked, sequential processes for polymerizing through to shaping, even for a polymeric material with poor processability such as high viscosity or high heat-sensitivity.
4. Manufacturing cost reduction due to the elimination of pelletizing and one-step melting.
5. Applicability to just-in-time production for various products.

Figure 7.29 shows a hybridized reactive extrusion and molding system, that is, the combination of an intermeshed twin screw extruder and forming equipment, such as injection molding, film making, etc. Experimental results that have been carried out for PP-PA-PPE ternary blending system are shown in Fig. 7.30. If this hybridized system is used, one can obtain a product with higher physical properties than conventional ones. Furthermore, this system can be fitted with an on-line monitoring device for the evaluation of physical properties of polymer alloys as shown in Fig. 7.31. The potential for a new type of production line for new polymer composites can be envisioned [46–51].

The morphological control as well as the initial reactive blending described in this chapter can be further utilized in the second stage of shaping or molding. The following is

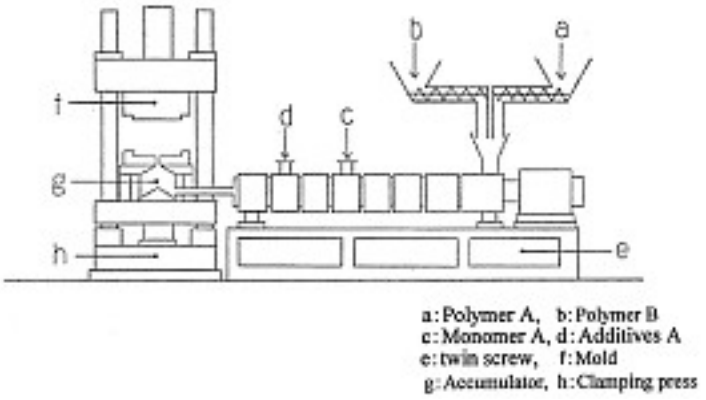

Figure 7.29 Combination of twin screw reactive extrusion and injection molding processes

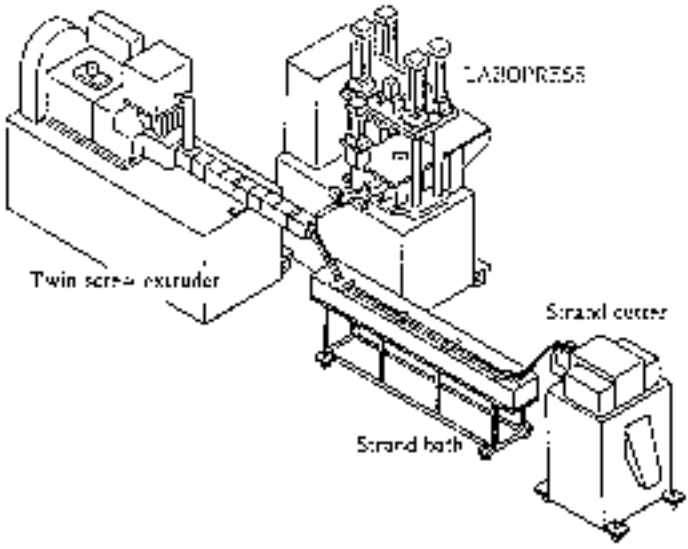

Figure 7.30 Application of small direct evaluation system for polymer alloys

an example of how to utilize it in injection molding. As-molded products with highly improved physical properties can be produced as shown in Fig. 7.32, because of the morphological optimization in the injection molding stage [52]. The improvement was brought about by the multi-phase morphology development along the thickness direction.

Figure 7.33 shows the morphological change from the surface to the center of the injection-molded product (thickness: 2 mm). To obtain better physical properties, the morphology has been optimized by means of the control of the viscosity-ratio of each polymer component and shear rate distribution in the mold. The concept for morphological optimization in injection molding is illustrated in Fig. 7.34.

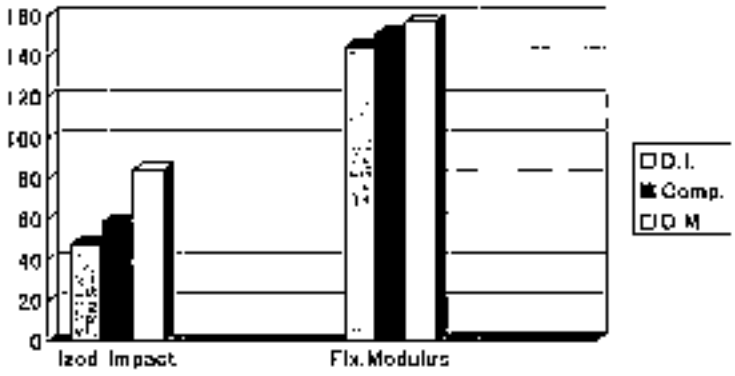

Figure 7.31 Improvement in product properties by a direct molding system. Impact: kgf cm/cm; Flex. Modulus: kgf/cm$_2$; DI: Direct feeding in injection molding machine; Comp.: Conventional compounding system; D.M.: Direct compounding and molding system

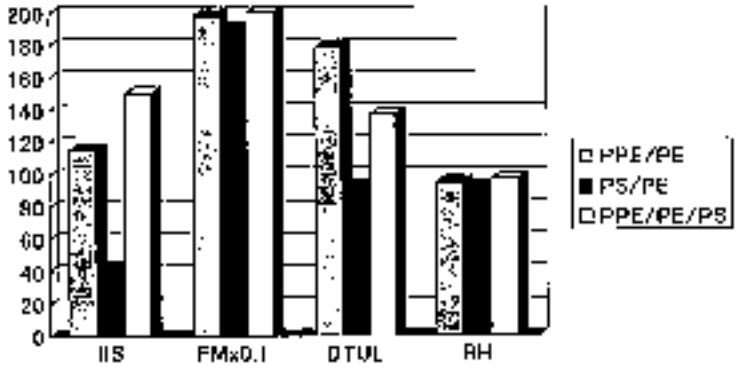

Figure 7.32 Mechanical and thermal properties of polyblends (PPE/PE/PS). IIS: Izod Impact Strength (J/m); FM: Flexural Modulus (Mpa); DTUL: Deflection Temp. (°C); RH: Rockwell Hardness (R-scale)

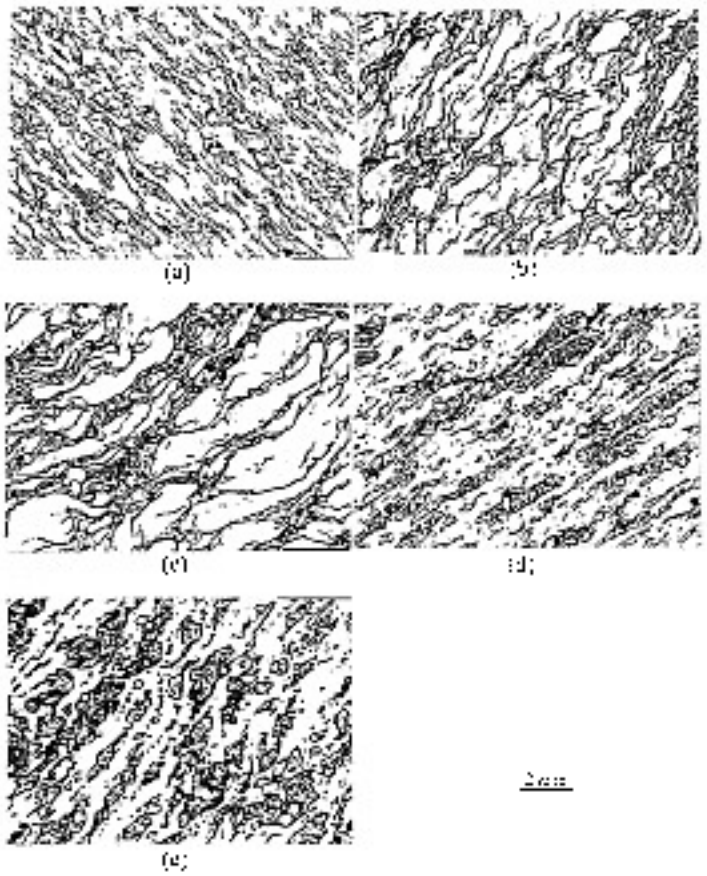

Figure 7.33 Transmission electron micrographs of various positions from surface of injection-molded sheet: (a) = 0.1 mm, (b) = 0.2 mm, (c) = 0.4 mm, (d) = 0.7 mm, (e) = 1.0 mm (center)

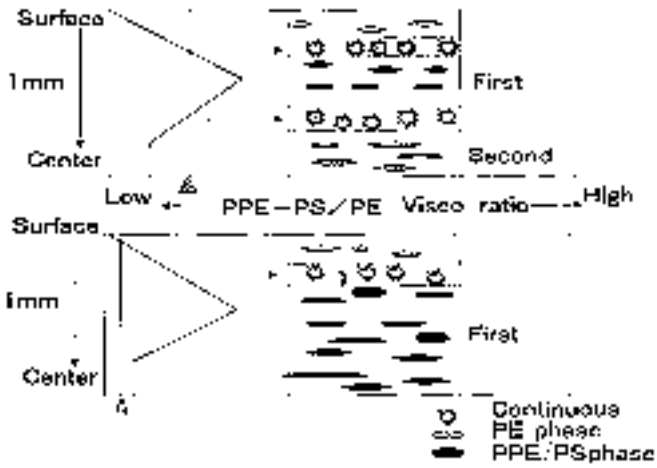

Figure 7.34 Phase inversion mechanism in injection-molded sheet

7.7 Conclusions

Screw type extruders have many advantages in reactive blending as follows:

- Continuous process for solid, powder, and liquid-form raw materials and reactants.
- Excellent distributive and dispersive mixing for high viscous fluids.
- Easy control of polymer temperature, pressure and residence time.
- No solvent requirement due to a bulk and melt-phase process.
- No special pre-processing requirement such as grafting reactions to provide functional groups in a raw material polymer.
- Removal of residual monomer and by-products from polymers.
- Self-wiping operation when closely-intermeshed twin screw and reciprocating single screw extruders are used.
- Consecutive process from chemical reactions, mixing, devolatilization to pelletizing and/or shaping.
- Many kinds of diversified polymer alloys can be produced with a single line.

Recently, new technologies to effectively control the morphological development during polymer processing have been advanced considerably for industrial use. To this end, good control techniques that make the best use of reactive processing are very important. In the near future, hybridized polymer processing systems, which combines reactive blending with other molding processes such as injection molding or blow molding, will become more common for creating innovative polymers with new functions and better properties such as synthetic biodegradable poly(lactic acid) [53].

References

1. T. Sakai, *Plastics Age*, April, 125 (1993).
2. T. Sakai, *Plastics Age*, February, 137 (1990).
3. T. Sakai, M.Mizoguchi, *Seikeikakou (Polymer Processing*), 3(6), 387 (1991).
4. J.L. White, Twin Screw Extrusion, Carl Hanser, Munich New York, 1990.
5. T. Sakai, 6th Polymer Processing Society Annual Meeting (Nice) (1990).
6. C. Rauwendaal, JSW Technical Report, No. 49, 3 (1993).
7. T. Sakai, N. Hashimoto, SPE ANTEC, Los Angeles, 157 (1987).
8. Werner & Pfleiderer Company ZSK, technical brochure.
9. W.D. Mohr, R.L. Saxton, *Industrial Engineering & Chemistry*, 49, 1855 (1957).
10. A.P. Plochoski, S.S. Dagli, *Polymer Engineering & Science*, 29(10), 617 (1989).
11. T. Sakai, *Kikaigakkai Ronbunshu(Mechanical Engineering),* 48(437), 156 (1982).
12. U. Burkhurt, H. Herrman, S.K. Jacopin, *Plastics Compounding*, Nov/Dec 73 (1978).
13. S. Ninomiya, Y. Nakano, T. Kajiwara, K. Funatu, JSW Technical Report, 49, 20 (1993).
14. Y. Nakano, S. Ninomiya, T. Kajiwara, K. Funatu, *Seikeikakou* (*Polymer Processing*), 5(8), 557 (1993).
15. G.I. Taylor, Proceeding Rheology Society. A138, 41 (1932), and A146, 501 (1934).
16. S. Wu, *J. Applied Science*, 35, 549 (1988).
17. S. Wu, *Polymer Engineering & Science*, 27(5), 335 (1987).
18. S. Wu, Polymer, 26, 1855 (1985).
19. G. Serpe, J. Jarrin, F. Dawans, *Polymer Engineering & Science*, 30 (9), 553 (1990).
20. U. Sundararaj, C.W. Macosko, C.K. Shih, SPE ANTEC 92, (Detroit) 1802 (1992).
21. L.A. Utracki, Z.H. Shi, *Polymer Engineering & Science*, 32(24), 1834 (1992).
22. H.P. Grace, Chemical Engineering Communication, 14, 225 (1982).
23. X.Q. Nuguyen, L.A. Utracki, US Patent 5, 451, 106 (1995).
24. T. Sakai, *International Polymer Processing*, V (4), 229 (1990).
25. T. Sakai, *Kikaigakkai Ronbunshu* (*Mechanical Engineering*), 48(446), 2078 (1983).
26. T. Sakai, *Kikaigakkai Ronbunshu* (*Mechanical Engineering*), 47(420), 156 (1981).
27. T. Sakai, *Kikaigakkai Ronbunshu* (*Mechanical Engineering*), 48(431), 1306 (1982).
28. S. Lim, J.L. White, *International Polymer Processing*, 8 (2), 119 (1993).
29. S. Lim, J.L. White, SPE ANTEC 93, (New Orleans) 2658 (1993).
30. C.E. Scott, C.W. Macosko, 7th Polymer Processing Society Annual Meeting (Hamilton), 102 (1991).
31. U. Sundararaj, C.W. Macosko, R. Rolando, *Polymer Engineering & Science*, 32 (24), 1814 (1992).
32. U. Sundararaj, C.W. Macosko, C.K. Shi, SPE ANTEC 92, (Detroit) 1802 (1992).
33. S. Bawiskar, J.L. White, *Polymer Engineering & Science*, 38 (5), 727 (1998).
34. J.T. Lindt, K. Ghosh, *Polymer Engineering & Science*, 32(24), 1802 (1992).
35. M.A. Huneault, Z.H. Shi, L.A. Utracki, Polyblends, 93 (Montreal) Oct. (1993).
36. H. Herrman, K. Eise, SPE ANTEC 39, 614, (1981).
37. T. Sakai, K. Nakamura, SPE ANTEC 88 (Atlanta), 1853 (1988).
38. T. Sakai, SPE ANTEC 86 (Boston) (1986).
39. T. Sakai, N. Hashimoto, K. Kataoka, International Polymer Processing VIII (3), 218 (1993).
40. N.H.Wang, T. Sakai, N. Hashimoto, International Polymer Processing X (4), 290 (1995).
41. T. Nishio, Y. Suzuki, M. Kakugo, *Koubunshi Ronbunshu* (*Polymer Science*), 47(4), 331 (1990).
42. T. Sakai, J. Kakizaki, K. Nakamura, 11th Polymer Processing Society Annual Meeting (Seoul), March (1995).
43. K. Okumura, T. Nishio, M. Kakugo, *Seikeikakou* (*Polymer Processing*), 3 (2), 108 (1991).
44. H. Sano, K. Yan, H. Ohi, K. Nishida, *Seikeikakou* (*Polymer Processing*), 6(11), 825 (1994).
45. C.G. Gogos, B. David, D.B. Todd, SPE ANTEC 93 (New Orleans), 1542 (1993).
46. T. Sakai, K. Nakamura, S. Inoue, SPE ANTEC 90, (Dallas), 1912(1990).
47. T. Sakai, K. Nakamura, S. Inoue, *International Polymer Processing*, VII (2), 117 (1992).
48. S. Inoue, K. Nakamura, T. Sakai, *Seikeikakou* (*Polymer Processing*), 4 (8), 484 (1992).
49. T. Sakai, K. Nakamura, S. Inoue, SPE ANTEC '91 (Montreal), 651 (1991).
50. T. Sakai, K. Nakamura, S. Inoue, *Polymer Engineering & Science* 33 (15), 989 (1993).

51. T. Sakai, *Seikeikakou* (*Polymer Processing*), 5(7), 465 (1993).
52. H. Sano, Y. Kurasawa, K. Nishida, *Kobunshi-Ronbunshu* (*Polymer Science*), 54 (4), 244 (1997).
53. R. Miyoshi, N. Hashimoto, Y. Sumihiro, K. Koyanagi, T. Sakai, *International Polymer Processing*, 11 (4), 320 (1996).